

1 **Convergent modeling of past soil organic carbon stocks but divergent projections**

2 Z. Luo¹, E. Wang¹, H. Zheng², J. A. Baldock³, O. J. Sun⁴, Q. Shao⁵

3 ¹ CSIRO Agriculture Flagship, GPO Box 1666, Canberra, ACT 2601, Australia.

4 ² CSIRO Land and Water Flagship, GPO Box 1666, Canberra, ACT 2601, Australia.

5 ³ CSIRO Agriculture Flagship, PMB 2, Glen Osmond, SA 5064, Australia.

6 ⁴ Institute of Forestry and Climate Change Research, Beijing Forestry University, Beijing 100083,

7 China.

8 ⁵ CSIRO Digital Productivity & Services Flagship, Private Bag 5, Wembley, WA 6913, Australia.

9 Correspondence to: Zhongkui Luo (zhongkui.luo@csiro.au) and Enli Wang (enli.wang@csiro.au).

10 **Abstract**

11 Soil carbon (C) models are important tool to understand soil C balance and project C stocks
12 in terrestrial ecosystems, particularly under global change. The initialization and/or
13 parameterization of soil C models can vary among studies even when the same model and
14 dataset are used, causing potential uncertainties in projections. Although a few studies have
15 assessed such uncertainties, it is yet unclear what these uncertainties are correlated with and
16 how they change across varying environmental and management conditions. Here, applying a
17 process-based biogeochemical model to 90 individual field experiments (ranging from 5 to 82
18 years of experimental duration) across the Australian cereal-growing regions, we
19 demonstrated that well-designed optimization procedures enabled the model to accurately
20 simulate changes in measured C stocks, but did not guarantee convergent forward projections
21 (100 years). Major causes of the projection uncertainty were due to insufficient understanding
22 of how microbial processes and soil C pool change to modulate C turnover. For a given site,
23 the uncertainty significantly increased with the magnitude of future C input and years of the
24 projection. Across sites, the uncertainty correlated positively with temperature, but negatively

25 with rainfall. On average, a 331% uncertainty in projected C sequestration ability can be
26 inferred in Australian agricultural soils. This uncertainty would increase further if projections
27 were made for future warming and drying conditions. Future improvement in soil C modeling
28 should focus on how microbial community and its C use efficiency change in response to
29 environmental changes, and better conceptualization of heterogeneous soil C pools and the C
30 transformation among those pools.

31 **1 Introduction**

32 Soil is the largest carbon (C) reservoir in the terrestrial biosphere and CO₂ emission from soil
33 organic matter (SOM) decomposition accounts for ~35% of the global CO₂ emissions
34 (Schlesinger and Andrews, 2000). Due to the large amount of soil organic carbon (SOC),
35 carbon sequestration in soils represents a great potential for mitigating greenhouse gas
36 emissions and climate change as well as maintaining soil fertility (Lal, 2004). Accurate
37 projections of future change in SOC are therefore needed for C and greenhouse gas (GHG)
38 inventories to guide the development of future policies and land management practices
39 (Janssens et al., 2003). Due to the complex and dynamic interactions between SOC, climate,
40 soil and land management practices, process-based SOM models have become an important
41 tool to investigate SOC change and project SOC trends under different land uses (Jenkinson
42 et al., 1991; Friedlingstein et al., 2006; Smith et al., 2007; Piao et al., 2009). Some studies
43 have suggested that the uncertainties in such projections should be systematically addressed
44 in order to judge the credibility of the underlying projections and develop appropriate policies
45 for carbon sequestration and climate change mitigation (Friedlingstein et al., 2006; Tang et al.,
46 2008; Todd-Brown et al., 2013; Nishina et al. 2014). Better understanding of these
47 uncertainties and their drivers will help identify knowledge gaps and improve process-based
48 models (Luo et al., 2014).

49 Uncertainty in simulation results derived from dynamic models can arise from inaccuracies in
50 input data, deficiencies in model structure and inappropriate optimization of model
51 parameters. For SOM models, initialization of the SOM pools can also be a major cause of
52 divergent model projections. Most SOM models divide SOM into several conceptual pools
53 (e.g. fast, slow and recalcitrant pools) and simulate the decomposition of each pool as a first-
54 order decay process (Smith et al., 1997; Davidson and Janssens, 2006; Schmidt et al., 2011).
55 In many cases, measurements are only available for total SOC, and there is no agreed-on
56 procedure for initialization of these model pools using total SOC (Basso et al., 2011). As a
57 result, model optimization was often conducted based on limited SOC measurements (usually
58 at temporal scales less than decades) together with empirical initialization. The optimized
59 model was then used to project SOC change at wider spatiotemporal scales (Friedlingstein et
60 al., 2006; Thornton et al., 2007). Such projection is subject to unknown uncertainty
61 (Friedlingstein et al., 2006; Tang et al., 2008; Luo et al., 2013), because it does not properly
62 address the inaccuracies in both model initialization and model parameters, with the latter
63 potentially caused by imperfect knowledge and model structure (Schmidt et al. 2011).

64 To illustrate the uncertainty propagation in SOC projections caused by initialization and
65 parameterization and to understand what correlates to the change in the patterns of projection
66 uncertainty, we used the Agriculture Production System sIMulator APSIM (Keating et al.,
67 2003; Wang et al., 2002; Holzworth et al., 2014) together with data from 90 agricultural
68 experiments at 26 sites across the Australian cereal-growing regions. The data include
69 measurements of total SOC stock (0–30 cm), C input (i.e., amount of residue retention), crop
70 yield, and records of management practices. The APSIM model uses a very similar SOM
71 pool structure and first decay approach to simulate SOM dynamics to other common Earth
72 system models (Smith et al., 1997; Friedlingstein et al., 2006; Thornton et al., 2007). We
73 firstly conducted sensitivity analysis to identify the model parameters whose change

74 impacted most on simulated SOC dynamics. We then used Bayesian optimization approach
75 to derive the posterior joint distribution of the identified parameters that enabled best match
76 between measured and observed SOC. These ensembles of parameters were used to run
77 APSIM for each of the 90 experiments, and simulations were continued for further 100 years
78 after the end of the experiment to produce SOC projections for uncertainty analysis. We
79 quantified the uncertainty in SOC projections induced by both initialization of SOC pools and
80 parameterization of algorithms for simulation of process dynamics. While the uncertainty
81 obviously increases with years of projections, we further hypothesized that it is also
82 influenced by site-specific climate, soil and management conditions, in addition to the impact
83 of model initialization and parameterization. We further investigated how the projection
84 uncertainty can be quantified by using these drivers, so that future SOC projections can
85 become more useful with attached and well quantified uncertainties.

86 **2 Materials and Methods**

87 2.1 Study sites and datasets

88 Data from a total of 90 experimental plots located within 26 different sites (Fig. 1 in the
89 supplement) and compiled and described by Skjemstad and Spouncer (2003) were used in
90 this study. The experimental duration of these trials ranged from 5 to 82 years, and cover
91 diverse climate, soil and agricultural management conditions and are representative of
92 Australian cereal-growing regions (Table 1 in the supplement). The dataset included detailed
93 records on crop sequence, crop yield, crop residue production (estimated according to harvest
94 index) and agricultural management practices such as residue management (removal or
95 retention) and fertilizer application over each year. SOC stock was determined for
96 representative 0-30 cm soil samples at least at the beginning and end of the each experiment,
97 with some experiments having as many as six temporal measurements. Other soil properties
98 at the start of the experiment were also measured including total nitrogen content, bulk

99 density, clay content and pH, and were used to initialize the APSIM model.

100 2.2 The APSIM model

101 APSIM was developed to simulate biophysical process in agricultural systems, and has been
102 comprehensively verified and used to study productivity, nutrient cycling and environmental
103 impacts of farming systems as influenced by climate variability and management practice
104 (Keating et al., 2003; Wang et al., 2002; Holzworth et al., 2014). APSIM simulates crop
105 growth and soil processes on a daily time-step in response to climate (i.e., temperature,
106 rainfall, and radiation) and soil conditions (water availability, and nutrient status etc.). The
107 model allows flexible specification of management options like crop and rotation type, tillage,
108 residue management, fertilization and irrigation. The ability of APSIM to simulate SOC
109 dynamics under different cropping and management practices has been verified (Probert et al.,
110 1998; Luo et al., 2011).

111 APSIM simulates the dynamics of both soil C and N stocks in each soil layer. Similar to other
112 SOM models like RothC and Century, SOM in APSIM is divided into six conceptual pools
113 (i.e., microbial biomass, humic organic matter and inert organic matter, together with three
114 fresh organic matter pools, Fig. 2 in the supplement). Inert organic matter is considered to be
115 non-susceptible to decomposition, i.e., indecomposable, due to physicochemical and/or
116 biological protections. The amount of inert organic C is initialized at the start of the
117 simulation and does not change during the simulation. The decomposition of other pools is
118 treated as a first-order decay process modified by soil temperature, moisture and nitrogen
119 availability (for fresh organic matter pool only), leading to the release of CO₂ to the
120 atmosphere and transfer of the remaining decomposed C to other pools. Microbial carbon use
121 efficiency (*CUE*), i.e., the efficiency of microbial community to assimilate the decomposed
122 SOC, determines the fraction of decomposed C transferred to other pools. The model

123 assumes a constant *CUE* for all C pools. The flow of N depends on the C:N ratio of the
124 receiving pool. The C:N ratio of each pool is assumed to be constant through time. The
125 decomposition of surface residues is modified by the degree of contact of the residue with
126 soil (Thorburn et al., 2001).

127 The model requires values for initial SOC content, total soil N content, bulk density, and soil
128 hydraulic parameters for each soil layer simulated. In the Skjemstad and Spouncer (2003)
129 dataset, measured values for SOC content, bulk density and total soil nitrogen content were
130 provided for the 0-30 cm layer. For the deeper soil layers and hydraulic parameters in the
131 whole soil profile, values from a measured soil profile nearest to the site were selected from
132 the Agricultural Production Systems Research Unit (APSRU) reference sites soil database
133 (<http://www.asris.csiro.au/mapping/hyperdocs/APSRU/>). Daily weather data (from 1889 to
134 present) for each site including radiation, maximum and minimum temperatures, and rainfall
135 was obtained from the SILO Patched Point Dataset
136 (<https://www.longpaddock.qld.gov.au/silo/>).

137 The APSIM model was first set up for each experiment. Agricultural management including
138 crops, residue management and fertilizer application was set according to available historical
139 records. Crops were sown depending on rainfall (>20 mm in successive five days) and soil
140 water content (90% of saturation water content in the top 20 cm soil). Crop cultivars were
141 assigned according to sowing date, i.e., the earlier the sowing date, the later the maturity type
142 of the crop cultivar. For simplification, three cultivars for each crop representing early,
143 middle and later maturity cultivars were selected from the default cultivars in the files
144 released with the APSIM model. For pasture, however, there was no record on the species
145 and cultivar. Here, perennial lucerne (*Medicago sativa*, a commonly used species in
146 Australian pasture) was used to represent pasture and only one cultivar—*trifecta*—was used in

147 the simulation. Lucerne was sown and removed after harvesting and before sowing of annual
148 crops in the corresponding rotations, respectively. Harvest to the height of 10 cm was
149 assumed each time lucerne reached the flowering stage to mimic possible grazing and/or
150 haying.

151 In the experiments included in this study, C from assimilation of crop growth was the only
152 source of C input to the soil. In the APSIM model, crop growth is simulated using light
153 interception and radiation use efficiency, modified by water and nitrogen supply. In order to
154 achieve credible simulation of crop growth, plant available water capacity (PAWC) of the
155 soil was adjusted. This adjusted PAWC at each site was used throughout the simulations.
156 Despite the reliability of the APSIM model to simulate crop growth (both belowground and
157 aboveground), we did not use the simulated aboveground C input during the simulation.
158 Alternatively, the recorded aboveground C input (as crop residue) was manually incorporated
159 into the model at the time of crop harvesting, whilst the simulated crop residue was removed.
160 This manipulation eliminated the effect of imperfect match of modeled with observed crop
161 residue on SOC dynamics.

162 2.3 Sensitivity analysis of SOC dynamics

163 A total of eight parameters (Table 2 in the supplement) that directly link to the SOC
164 dynamics in the model were selected for sensitivity analysis in order to identify the most
165 important ones regulating SOC dynamics. One model input for model initialization, i.e., the
166 fraction of inert organic carbon in the total SOC at the start of the simulation (*finert*), was
167 also included in the sensitivity analysis, due to lack of observed data of *finert* and its great
168 effect on simulated soil C changes. To inspect the response of simulated SOC to variations of
169 those parameters (*finert* was also called as a parameter for convenience hereafter), a
170 univariate local sensitivity analysis was conducted by looking at the impact of one parameter

171 at a time and fixing all other parameters. As the purpose was to identify the most influential
 172 parameter(s), a continuous wheat system with 100% residue retention (the dominant crop in
 173 the studied experiments, see Table 1 in the supplement) and a nitrogen application of 200 kg
 174 N ha⁻¹ yr⁻¹ were used and simulated for 100 years. The default model parameters were first
 175 used (Table 2 in the supplement), and then each parameter was sequentially increased by 10%
 176 of its default value. For each parameter, the sensitivity function (S_i) was calculated to
 177 represent the sensitivity of model output y (i.e., total 0-30 cm SOC stock) to changes in a
 178 single parameter θ_i (Soetaert and Herman, 2008):

$$179 \quad S_i = \theta_i \frac{y|_{\theta_i^*} - y|_{\theta_i}}{\theta_i^* - \theta_i}, \quad (1)$$

180 where θ_i was the default parameter value, and $y|_{\theta_i}$ the model output using θ_i , θ_i^* the altered
 181 parameter value (increased by 10%) and $y|_{\theta_i^*}$ the model output using θ_i^* . Finally, the
 182 importance index of the i^{th} parameter (I_i), i.e., the overall sensitivity of the output with respect
 183 to this parameter, was calculated by summarizing the sensitivities for the 100 year outputs
 184 ($n=100$):

$$185 \quad I_i = \sqrt{\frac{1}{n} \sum_{j=1}^n S_{ij}^2}. \quad (2)$$

186 where S_{ij} was the sensitivity function for parameter i at the j^{th} year of the n ($n = 100$) years of
 187 each simulation. The greater the magnitude of I is, the more sensitive the model output was to
 188 the parameter (Soetaert and Herman, 2008). The importance indices were compared among
 189 the nine parameters, and the most important parameters were identified and optimized to
 190 obtain the best agreement between simulated and observed SOC dynamics for each of the 90
 191 experiments. As the relative importance of those parameters was independent of soil and
 192 climate conditions, the typical soil and climate at Wagga Wagga (a major cropping area in
 193 Australia, and one of the 26 sites used in the main text), New South Wales of Australia were

194 selected to conduct above analyses.

195 2.4 Model optimization

196 The differential evolution (DE) algorithm (belongs to the class of genetic algorithms) was
197 used to optimize the most influential parameters identified. The optimization was performed
198 in R 3.0.3 using the DEoptim function in the “DEoptim” package (Mullen et al., 2011). DE is
199 a global optimization algorithm for continuous numerical minimization problems, which use
200 biology-inspired operations of crossover, mutation, and selection on population in order to
201 minimize an objective function over the course of successive generations.

202 To use DE, each parameter was first assumed to exhibit a uniform distribution bounded
203 within a range (i.e., the prior distribution, see Table 2 in the supplement) that was
204 biologically and physically possible based on previous knowledge about the process, thereby
205 eliminating solutions in conflict with prior knowledge. The optimization performed a quasi-
206 random walk through the multi-dimensional parameter space to find the parameter set that
207 caused the model to generate the best match between predicted and observed SOC. The “best
208 match” was defined as the model output that minimized the criteria selected for model
209 evaluation (Table 3 in the supplement). Seven criteria that are commonly used in the
210 literature were selected to assess the possible effects of criterion selection on modeling results.
211 Using each criterion, the optimization was conducted 100 times (i.e., 100 ensembles of initial
212 parameter values through quasi-random walk), which generated 100 ensembles of parameters
213 (i.e., the joint posterior distribution of the most influential parameters), giving simulation
214 results with approximately equally good matches to the observed data. Consequently, 700
215 ensembles of parameters (from using seven criteria) for each experiment were produced. The
216 optimizing procedure and related simulations were operated on Bragg and Dell CPUs of
217 CSIRO Clusters.

218 However, the required computing time (~2 days for one experiment and one selection
219 criterion using 100 computer cores) has posed a significant challenge even using the high
220 performance computing clusters (Bragg and Dell CPUs) for this multi-parameter optimization
221 of the process-oriented APSIM model. To complete all optimizations using seven criteria for
222 the 90 experiments, a run time of four months was expected assuming that 1000 cores could
223 be continuously available on the clusters. For this reason, the global optimization DE was
224 only applied for two sites, i.e., Brigalow and Tarlee, providing two cases of DE optimization
225 as compared to an alternative and faster Bayesian sampling approach as described below.

226 For all the experiments, a Bayesian sampling approach was substituted for the DE
227 optimization in order to complete the work within a reasonable time but without much
228 sacrificing of model performance. The APSIM model was run for each experiment for
229 100,000 times using 100,000 ensembles of parameters that were randomly sampled from their
230 prior distributions. The best 100 ensembles of parameters were selected as their posterior
231 distributions through using each criterion listed in Table 3 in the supplement. At Brigalow
232 and Tarlee, the distributions of parameters “optimized” through this Bayesian sampling
233 approach were compared with those optimized through DE optimization. The identified
234 parameter ensembles by Bayesian sampling approach were referred to as “optimized
235 parameters” in the following text and used to assess the uncertainty in projected SOC.

236 2.5 Uncertainty in projected SOC

237 After obtaining the 700 ensembles of optimized parameters (i.e., after “optimization period”),
238 the APSIM model was run continuously from the start to the end of each experiment and then
239 for an additional 100 years after the end of each experiment using each parameter set (i.e.,
240 700 simulations for each experiment). For the last 100-year simulations (i.e., projection
241 period), a continuous wheat system was assumed together with 100% residue retention,

242 which is the same as that used in sensitivity analysis. Carbon input through crop residue
243 retention was expected to be an important factor regulating SOC dynamics in the projection
244 period. As residue (or biomass) production is dominantly controlled by fertilizer application
245 rates under natural rainfall condition at each site, scenarios with nitrogen application rates
246 ranging from 0 to 300 kg N ha⁻¹ yr⁻¹ with increment of 20 kg N ha⁻¹ yr⁻¹ were modeled.
247 These scenarios made it possible to mimic different management practices that influence C
248 input to the soil and to assess its impact on the uncertainty of simulated SOC induced by
249 model initialization and parameterization.

250 Climate data from the start year of each experiment through to 2013 was used for the
251 corresponding simulation period. For all years from 2014 onwards, the corresponding years
252 of the latest historical climate data were used. For example, for the possible simulations from
253 2014 to 2104 (91 years), the historic climate data of 91 years from 1923 to 2013 was used. As
254 we focused on the potential uncertainty induced by model parameterization and initialization,
255 we did not consider the uncertainty related to climate change.

256 SOC content in the 0-30 cm soil layer was output at the start of projection (excluding the
257 optimization period) and at the end of each year of projection (C_i). For the i^{th} year of
258 projection, the mean (M_{SOC_i}) of C_i of the 700 estimates was calculated, and the range (R_{SOC_i})
259 of the 95% confidence interval was calculated as the difference between 97.5th and 2.5th
260 percentile of the 700 estimates. Then, the percentage uncertainty (U_{P_i}) for that year of
261 projection was estimated based on half of the R_{SOC_i} divided by the M_{SOC_i} :

$$262 \quad U_{P_i} = \frac{R_{\text{SOC}_i}}{2 \times M_{\text{SOC}_i}} \times 100\%, i = 1, 2, 3, \dots, 100. \quad (3)$$

263 2.6 Attributes controlling the variability of the uncertainty

264 After estimating U_P , we further addressed the following question: how and why does the

265 uncertainty (i.e., U_P) in projected SOC change across space and time? We hypothesized that
 266 U_P is associated with the management in terms of residue C inputs. At the same time, we
 267 assumed that the detailed relationship between U_P and C inputs is different not only across
 268 experiments but also across time periods of the projection. As the hierarchy of the
 269 relationships (i.e., individual-level C inputs group in experiments and time periods of the
 270 projection), a hierarchical regression model, also called multilevel model (Gelman and Hill,
 271 2006), was fitted to estimate U_{Pi} (y_i) on C input (x_i), applied to the $J = 90$ experiments and K
 272 $= 100$ time periods of projection. The multilevel model was written as a data (the predicted
 273 U_{Pi} belonging to experiment j with k years of projection) level model, allowing the model
 274 coefficients (α and β) to vary by experiment ($j = 1, \dots, J$) and time period of projection ($k =$
 275 $1, \dots, K$) (Gelman and Hill, 2006):

$$276 \quad y_i \sim N(\alpha_{j[i],k[i]} + \beta_{j[i],k[i]}x_i, \sigma_y^2), \text{ for } i = 1, \dots, n, \quad (4)$$

277 and a decomposition of its intercepts and slopes into terms for experiment, the time period of
 278 projection and their interaction,

$$279 \quad \begin{pmatrix} \alpha_{j,k} \\ \beta_{j,k} \end{pmatrix} \sim \begin{pmatrix} \alpha_j^{\text{expt}} + \alpha_k^{\text{year}} + \alpha_{j,k}^{\text{expt} \times \text{year}} \\ \beta_j^{\text{expt}} + \beta_k^{\text{year}} + \beta_{j,k}^{\text{expt} \times \text{year}} \end{pmatrix} + \begin{pmatrix} \gamma_{0j}^{\text{expt}} \\ \gamma_{1j}^{\text{expt}} \end{pmatrix} + \begin{pmatrix} \gamma_{0k}^{\text{year}} \\ \gamma_{1k}^{\text{year}} \end{pmatrix} + \begin{pmatrix} \gamma_{0jk}^{\text{expt} \times \text{year}} \\ \gamma_{1jk}^{\text{expt} \times \text{year}} \end{pmatrix}, \quad (5)$$

280 and models for variation,

$$281 \quad \begin{pmatrix} \gamma_{0j}^{\text{expt}} \\ \gamma_{1j}^{\text{expt}} \end{pmatrix} \sim N \left(\begin{pmatrix} 0 \\ 0 \end{pmatrix}, \Sigma^{\text{expt}} \right), \text{ for } j = 1, \dots, J \quad (6)$$

$$282 \quad \begin{pmatrix} \gamma_{0k}^{\text{year}} \\ \gamma_{1k}^{\text{year}} \end{pmatrix} \sim N \left(\begin{pmatrix} 0 \\ 0 \end{pmatrix}, \Sigma^{\text{year}} \right), \text{ for } k = 1, \dots, K \quad (7)$$

$$283 \quad \begin{pmatrix} \gamma_{0jk}^{\text{expt} \times \text{year}} \\ \gamma_{1jk}^{\text{expt} \times \text{year}} \end{pmatrix} \sim N \left(\begin{pmatrix} 0 \\ 0 \end{pmatrix}, \Sigma^{\text{expt} \times \text{year}} \right), \text{ for } j = 1, \dots, J; k = 1, \dots, K. \quad (8)$$

284 where Σ was the 2×2 covariance matrix representing the variation of the intercepts and slopes
285 in the population of groups (experiments and time periods of projection). In essence, there is
286 a separate regression model for each experiment and time period combination with the
287 coefficients estimated by the weighted average of pooled (do not consider groups) and un-
288 pooled (consider each group separately) estimates, i.e., partial pooling. This hierarchical
289 structure of the model allows the assessment of the variation of individual-level coefficients
290 across groups and accounting for group-level variation in the uncertainty for individual-level
291 coefficients.

292 To assess the variation of individual-level coefficients (α_j^{expt} and β_j^{expt}) across different
293 experiments, a classic linear regression was conducted to identify the effects of different
294 sources of variation. At the experiment level, we assumed that two groups of attributes
295 influence α_j^{expt} and β_j^{expt} : 1) uncertainty in model parameters, i.e., the three optimized
296 parameters based on experiment-specific dataset, and 2) climate including mean annual
297 rainfall and temperature, which are predominant factors controlling SOC dynamics during
298 model optimization as well as during projection. The generalized variance (GV) was
299 calculated as an indicator of the overall variation in model parameters, which is defined as the
300 determinant of the variance-covariance matrix of the three parameters and is a scalar measure
301 of overall multidimensional scatter. The two groups of attributes including all interactions
302 were selected through a stepwise regression model selection by Akaike Information Criterion.
303 Before fitting the model, GV was logarithmically transformed to satisfy additivity and
304 linearity assumptions and then centered by subtracting the mean of the data, and rainfall and
305 temperature were also centered. For coefficients over the time-spans of projection (α_k^{year} and
306 β_k^{year}), their relationship with the time-span of projection were presented. All the statistical
307 analyses including the multilevel model fitting were conducted using the R software version

308 3.0.3 (R Core Team, 2013).

309 **3 Results and discussion**

310 3.1 Sensitivity analysis and model performance

311 Three parameters were identified as most influential on simulated SOC (Fig. 3 in the
312 supplement). Microbial carbon use efficiency (*CUE*) had the biggest impact. This highlights
313 the key role of microbial process to control SOM decomposition, and the need for better
314 capturing the dynamics and impact of microbial process in SOM models (Allison et al., 2010;
315 Singh et al., 2010; Sinsabaugh et al., 2013; Xu et al., 2014). As *CUE* was treated as a
316 constant in most SOM models, a framework is needed to incorporate microbial data (e.g.,
317 community, activity, and their responses and feedbacks to biotic and abiotic factors) into
318 SOM models to provide robust estimations and predictions. Potential decomposition rate
319 constant of humic organic matter (k_{hum} , day⁻¹) ranked the second, followed by the fraction of
320 the humic carbon that is recalcitrant to decomposition (*finert*). This result further indicates the
321 importance to better quantify the decomposability of the heterogeneous SOM (Schmidt et al.,
322 2011; Sierra et al., 2011). It should be noted that the actual decomposition rate is simulated
323 through modifying k_{hum} by a series of biotic and abiotic variables at different spatiotemporal
324 scales, and different models simulate the responses differently (Todd-Brown et al, 2013;
325 Exbrayat et al., 2014). Although we did not quantify the relative importance of these
326 modifiers (e.g., soil moisture and temperature), the results indicated that k_{hum} has to be
327 constrained, implying the importance of determining how it responds to environmental
328 factors. The wide distributions of *CUE*, k_{hum} and *finert* parameters (derived by constraining
329 the model against the measurement data, Fig. 1b) imply deficiencies in our understanding of
330 the microbial community and its activity and how they change with environmental conditions
331 to modulate the SOM decomposition processes.

332 Our optimization procedure enabled accurate simulation of SOC change during the
333 optimization period (Fig 1a) using distinct ensembles of model parameters for each
334 experiment (Fig. 1b). Pooling together all data of the 90 experiments, the modeled average
335 SOC of the 700 simulations could explain 96% ($P < 0.001$) of the variance in observed SOC
336 (Fig. 1a). For each experiment, model performance was nearly identical (Fig. 1a) when the
337 simulations (using different parameter sets) were inter-compared. At the Tarlee site (Fig. 2a),
338 for example, the RMSE between modeled and observed SOC ranged from 0.44 to 0.52 t ha⁻¹,
339 compared with the range of 3.11 to 3.12 t ha⁻¹ at Brigalow site (Fig. 2b). This high level of
340 consistency highlights significant equifinality, i.e., different parameter ensembles leading to
341 similar simulation results (Fig 1b, 2c and 2d), in process-based SOM models, which must be
342 addressed in modeling studies aimed at enhanced process understanding and hypothesis
343 testing (Tang et al., 2008; Luo et al., 2011).

344 3.2 Uncertainty in SOC projections

345 The accurate simulations of past SOC, however, do not guarantee convergent projections
346 beyond the model optimization period. In contrast, running the model with the same
347 parameter ensembles generated very divergent future projections (Fig. 2a and b), indicating
348 significant uncertainty propagation with time of projection (Luo et al., 2011; Tang et al.,
349 2008). Furthermore, the uncertainty is also related to management in terms of C input level
350 and site conditions. At Brigalow (Fig. 2b), for example, the 95% confidence interval of
351 projected SOC under optimal N input (i.e., no N stress for crops) ranged from 37 to 56 t ha⁻¹
352 10 years after the model optimization period, which increased to 26–68 t ha⁻¹ for the
353 projected SOC after 50 years. Under low N input scenario (0 kg N ha⁻¹), the uncertainty was
354 smaller. At Tarlee (Fig. 2a), the uncertainty propagation followed a similar pattern to that at
355 Brigalow, but the uncertainty under low N input scenario was much smaller. At Brigalow, in
356 addition, we found that the choice of criterion (objective functions) influenced the

357 distributions of the derived parameters (Fig. 2d) because a specific criterion only focuses on a
358 specific aspect (e.g., mean or variance) of the data and the model results, of which the
359 consequence for SOC simulations (e.g., the bifurcation pattern of projected SOC showed in
360 Fig. 2b) ought to be carefully considered in future studies.

361 It is important to notice that the posterior distributions of model parameters were apparently
362 different across experiments (Fig. 1b, c and d, and Fig. 4 in the supplement), confirming that
363 model parameters are sensitive to the data constraining the model (Keenan et al., 2012;
364 Hararuk et al., 2014; Luo et al., 2014). Our results indicate that *CUE* was likely higher for
365 site under longer cultivation history (the Tarlee site) than for new-cleared site (the Brigalow
366 site, Fig 2c vs 2d), implying the potential importance of land use history for constraining
367 model parameters such as microbial carbon use efficiency because land use history has direct
368 effect on the quantity and quality of carbon input as well as on soil properties. However, such
369 impact needs further confirmation with more data. The distributions of the optimized model
370 parameters were also influenced by the choice of criteria to evaluate model performance (Fig.
371 2d, Fig. 5 in the supplement). The differences in parameter distributions subsequently impact
372 on the SOC projections as showed in Fig. 2b, albeit the near identical model performance in
373 simulating historical SOC. In addition, *finert* and *k_{hum}* was positively related (Fig. 2c and d),
374 implying the importance of the interactions and/or feedback between different C pools and
375 their impacts on soil C projection. These highlight the needs for: 1) improving the science for
376 capturing process interactions in the model such as the role of microbial processes and
377 conceptualization of heterogeneous C pools and their transformation (Manzoni et al., 2012;
378 Luo et al., 2014), 2) conducting model optimization conditioned on all observed data from
379 experiments together with Bayesian inference technique, and 3) quantifying uncertainty in
380 SOC projections with ensemble model simulations (Post et al., 2008; Weng et al., 2011; Xia
381 et al., 2013; Hararuk et al., 2014; Luo et al., 2014).

382 If a continuous wheat system was practiced for 100 years after the end of each experiment at
383 the 26 sites, optimal N management was predicted to result in an average increase in SOC
384 (Fig. 3a), while a SOC decline under zero N input (Fig. 3b). The amount of potential SOC
385 change depends on not only the management level (N input) and the climate and soil
386 conditions that determine the potential productivity of crops, but also the initial SOC level at
387 the start of the projections. Across the 90 experiments, the percentage uncertainty in the SOC
388 projections ranged from 2% to 140% with an average of 53% under optimal N management
389 (Fig. 3c), and from 0.8% to 108% with an average of 40% under zero N input (Fig. 3d).
390 Applying this result to Australia's cereal-growing regions, the simulated potential SOC stock
391 of ~7.5 Pg (Luo et al., 2013) could be subject to 53% uncertainty under no N deficient and
392 100% residue retention.

393 3.3. Attributes controlling the variability of the uncertainty

394 The uncertainty propagation with time of prediction and across experiments could be
395 explained using a linear model by linking the percentage uncertainty (U_P) to the C input from
396 crop residue (C_R), i.e., $U_P = \alpha + \beta C_R$. However, both α and β changed significantly across
397 experiments (Fig. 4a) and years of projections (Fig. 4b), and were also impacted by their
398 interactions. Across the time periods of projection, the uncertainty increased with the number
399 of years for projection, reflected by the linear increase in α (model intercepts) and asymptotic
400 increase in β (model slope, Fig. 4b). The asymptotic increase in β (model slope) also implies
401 that the relative contribution of C input to prediction uncertainty reduces with time. Across
402 experiments, there was a marked variation in the effect of C input on U_P , indicating impact of
403 site-specific conditions (e.g. climate and soil as described later). Across sites and years of
404 projections, the majority of positive β implies increased uncertainty in SOC projections with
405 increasing C input, which has not been properly addressed in previous modeling studies (Joos

406 et al., 2001; Jones et al., 2005; Smith et al., 2005; Ogle et al., 2010). The fate of C input has
407 direct effect on the amount of soil C. The general positive effect of C input on uncertainty
408 would attribute to that the amount of C input ending up in the soil would be more variable
409 and thus higher uncertainty in soil C under higher C input. These results highlight the
410 importance of understanding the consequences of future C input changes on soil C dynamics.

411 The variance in model parameters (GV) across experiments had a major effect on the
412 intercepts (positive at $P < 0.001$) and slopes (positive at $P < 0.001$) of the regression model
413 linking U_P to C input (Table 1). As GV was logarithmically transformed when fitting the
414 model, the increase in U_P with GV was exponential across experiments. This result highlights
415 the crucial role to improve the representation of the sensitive microbial processes (Zhou et al.,
416 2012; Xu et al., 2014) and the heterogeneous SOM (Sierra et al., 2011) in biogeochemical
417 SOM models, and to constrain the space of relevant model parameters. For example, we
418 assumed a relatively wide range of *CUE* (0.2–0.8) as the prior information for the Bayesian
419 optimization. Sinsabaugh et al. (2013) suggested that *CUE* prediction should consider
420 resource composition, stoichiometry constraints and biomass composition, as well as
421 environmental drivers. A more informative prior of *CUE* could help reduce the uncertainty in
422 soil C projections.

423 Rainfall and temperature, together with their interaction, had significant impact on SOC
424 projection uncertainty through their impact on the fitted model intercepts across experiments
425 (Table 1). α_j^{expt} increased with temperature, but tended to decrease with rainfall, implying
426 increased uncertainty in SOC projection under future warming and drying conditions. Based
427 on the results, the uncertainty in projected SOC will be increased by 4.95%, if average
428 temperature is increased by 1 °C under global warming. For the slopes β_j^{expt} , rainfall and its
429 interaction with GV had significant negative effect. These effects may reflect the impact of

430 rainfall on both primary productivity (thus C input) and soil moisture conditions (thus
431 microbial activity and decomposition rate of SOC), emphasizing the importance of
432 understanding the interactions between soil processes and their responses to external drivers
433 and management such as temperature and rainfall (Davidson and Janssens, 2006; Carvalhais
434 et al., 2014).

435 **4 Conclusions**

436 Our results demonstrate that great uncertainty exists in soil C projections from process-based
437 SOM models, due to deficiency in model initialization and parameterization to capture the
438 process interactions, such as microbial C use efficiency and its drivers, as well as lack of
439 detailed information to initialize the model, e.g., the heterogeneous SOM with different
440 decomposability. The prediction uncertainty propagates with extended years of projections
441 and C input into soil. It is also influenced by site-specific climate (temperature and rainfall)
442 and soil conditions together with management inputs, which determine both the C input
443 (through primary productivity) and the SOM decomposition processes. The results also
444 suggest that C projection into warming and drying future climate will be subject to even
445 increased uncertainty. For agricultural land uses, uncertainty caused by management practices
446 has to be carefully considered due to its impact on microbial activity and subsequent
447 projected SOC. For any future predictions of SOC change, ensemble simulations conditioned
448 on total observed datasets together with a Bayesian inference technique should be used in
449 order to quantify the uncertainties in modeling results. Based on our results, future
450 improvement in SOM modeling should focus on how microbial community and its carbon
451 use efficiency change in response to environmental changes, better quantification of
452 heterogeneous SOM and the effects of its change on total soil C turnover.

453 **Author contributions**

454 Z.L collected data, run simulations, and performed data analysis; Z.L, E.W., J.B. designed the
455 study; H.Z. and Q.S. was involved in statistical analysis; Z.L., E.W. and O.J.S. wrote the
456 paper. All authors discussed the results and commented on the manuscript.

457 **Acknowledgements**

458 This study was supported by funding from the Australian Government Department of
459 Agriculture, Fisheries and Forestry (DAFF) and the Grain Research and Development
460 Corporation (GRDC). Thanks to Dr. Yiqi Luo of the University of Oklahoma, Dr. Petra
461 Kuhnert and Dr. Jonathan Sanderman of CSIRO for their helpful comments on an earlier
462 version of the manuscript.

463 **References**

- 464 Allison, S. D., M. D. Wallenstein, and M. A. Bradford (2010), Soil-carbon response to
465 warming dependent on microbial physiology. *Nature Geoscience*, **3**, 336-340.
- 466 Basso, B., O. Gargiulo, K. Paustian, G. P. Robertson, C. Porter, P. Grace, and J. W. Jones
467 (2011), Procedures for initializing soil organic carbon pools in the DSSAT-CENTURY
468 model for agricultural systems. *Soil Science Society of American Journal*, **75**, 69-78.
- 469 Carvalhais, N., M. Forkel, M. Khomik et al. (2014), Global covariation of carbon turnover
470 times with climate in terrestrial ecosystems. *Nature*, **514**, 213-217.
- 471 Davidson, E. A., and I. A. Janssens (2006), Temperature sensitivity of soil carbon
472 decomposition and feedbacks to climate change. *Nature*, **440**, 165-173.
- 473 Exbrayat, J. F., A. J. Pitman, and G. Abramowitz (2014), Response of microbial
474 decomposition to spin-up explains CMIP5 soil carbon range until 2100 *Geosci. Model*
475 *Dev.* **7**, 2683–2692
- 476 Friedlingstein, P., P. Cox, R. Betts et al. (2006), Climate-carbon cycle feedback analysis:
477 Results from the (CMIP)-M-4 model intercomparison. *Journal of Climate*, **19**, 3337-3353.

478 Gelman, A., and J. Hill (2006), Data analysis using regression and multilevel/hierarchical
479 models. (Cambridge University Press).

480 Hararuk, O., J. Y. Xia, and Y. Q. Luo (2014), Evaluation and improvement of a global land
481 model against soil carbon data using a Bayesian Markov chain Monte Carlo method.
482 Journal of Geophysical Research-Biogeoscience, **119**, 403-417.

483 Holzworth, D. P., N. Huth, P. G. deVoil, E. J. Zurcher, H. I. Herrmann, G. McLean, K.
484 Chenu, E. J. van Oosterom, V. Snow, C. Murphy, A. D. Moore, H. Brown, J. P. M. Whish,
485 S. Verrall, J. Fainges, L. W. Bell, A. S. Peake, P. L. Poulton, Z. Hochman, P. J. Thorburn,
486 D. S. Gaydon, N. P. Dalgliesh, D. Rodriguez, H. Cox, S. Chapman, A. Doherty, E.
487 Teixeira, J. Sharp, R. Cichota, and I. Vogeler (2014), APSIM-Evolution towards a new
488 generation of agricultural systems simulations. Environmental Modelling & Software, **62**,
489 327-350.

490 Janssens, I. A., A. Freibauer, P. Ciais et al. (2003), Europe's terrestrial biosphere absorbs 7 to
491 12% of European anthropogenic CO₂ emissions. Science, **300**, 1538-1542.

492 Jenkinson, D., D. Adams, and A. Wild (1991), Model estimates of CO₂ emissions from soil in
493 response to global warming. Nature, **351**, 304-306.

494 Jones, C., C. McConnell, K. Coleman, P. Cox, P. Falloon, D. Jenkinson, and D. Powlson
495 (2005), Global climate change and soil carbon stocks; predictions from two contrasting
496 models for the turnover of organic carbon in soil. Global Change Biology, **11**, 154-166.

497 Joos, F., I. C. Prentice, S. Sitch, R. Meyer, G. Hooss, G. K. Plattner, S. Gerber, and K.
498 Hasselmann (2001), Global warming feedbacks on terrestrial carbon uptake under the
499 Intergovernmental Panel on Climate Change (IPCC) emission scenarios. Global
500 Biogeochemical Cycles **15**, 891-907.

501 Keating, B. A., P. S. Carberry, G. L. Hammer et al. (2003), An overview of APSIM, a model
502 designed for farming systems simulation. European Journal of Agronomy, **18**, 267-288.

503 Keenan, T. F., E. Davidson, A. M. Moffat, W. Munger, and A. D. Richardson (2012) Using
504 model-data fusion to interpret past trends, and quantify uncertainties in future projections,
505 of terrestrial ecosystem carbon cycling. *Global Change Biology*, **18**, 2555-2569 (2012).

506 Lal, R. (2004), Soil Carbon sequestration impacts on global climate change and food security.
507 *Science*, **304**, 1623-1627.

508 Luo, Y., K. Ogle, C. Tucker, S. Fei, C. Gao, S. LaDeau, J. Clark, and D. S. Schimel (2011),
509 Ecological forecasting and data assimilation in a data-rich era. *Ecological Applications*,
510 **21**, 1429-1442.

511 Luo, Y., T. F. Keenan, and M. Smith (2014), Predictability of the terrestrial carbon cycle.
512 *Global Change Biology*, DOI: 10.1111/gcb.12766.

513 Luo, Z., E. Wang, B. A. Bryan, D. King, G. Zhao, X. Pan, U. Bende-Michl (2013), Meta-
514 modeling soil organic carbon sequestration potential and its application at regional scale.
515 *Ecological Applications*, **23**, 408-420.

516 Luo, Z., E. Wang, O. J. Sun, C. J. Smith, and M. E. Probert (2011), Modeling long-term soil
517 carbon dynamics and sequestration potential in semi-arid agro-ecosystems. *Agricultural
518 and Forest Meteorology*, **151**, 1529-1544.

519 Luo, Z., E. Wang, I. R. P. Fillery, L. M. Macdonald, N. Huth, and J. Baldock (2014),
520 Modelling soil carbon and nitrogen dynamics using measurable and conceptual soil
521 organic matter pools in APSIM. *Agriculture, Ecosystems & Environment*, **186**, 94-104.

522 Manzoni, S., P. Taylor, A. Richter, A. Porporato, and G. I. Ågren (2012), Environmental and
523 stoichiometric controls on microbial carbon use efficiency in soils. *New Phytol.*, **196**, 79-
524 91.

525 Mullen, K.M., D. Ardia, D. L. Gil, D. Windover, and J. Cline (2011), DEoptim: An R
526 package for global optimization by differential evolution. *Journal of Statistical Software*,
527 **40**, 6.

528 Nishina, K., Ito, A., Beerling, D. J., Cadule, P., Ciais, P., Clark, D. B., Falloon, P., Friend, A.
529 D., Kahana, R., Kato, E., Keribin, R., Lucht, W., Lomas, M., Rademacher, T. T., Pavlick,
530 R., Schaphoff, S., Vuichard, N., Warszwaski, L., and Yokohata, T. (2014) Quantifying
531 uncertainties in soil carbon responses to changes in global mean temperature and
532 precipitation. *Earth System Dynamics*, **5**, 197–209.

533 Ogle, S. M., F. J. Breidt, M. Easter, S. Williams, K. Killian, and K. Pautian (2010), Scale and
534 uncertainty in modeled soil organic carbon stock changes for US croplands using a
535 process-based model. *Global Change Biology*, **16**, 810-822.

536 Piao, S. L., J. Y. Fang, P. Ciais, P. Peylin, Y. Huang, S. Sitch, and T. Wang (2009), The
537 carbon balance of terrestrial ecosystems in China. *Nature*, **458**, 1009-1013.

538 Post, J., F. F. Hattermann, V. Krysanova, and F. Suckow (2008), Parameter and input data
539 uncertainty estimation for the assessment of long-term soil organic carbon dynamics.
540 *Environmental Modelling and Software*, **23**, 125-138.

541 Probert, M., J. Dimes, B. Keating, R. Dalal, W. Strong (1998), APSIM's water and nitrogen
542 modules and simulation of the dynamics of water and nitrogen in fallow systems.
543 *Agricultural Systems*, **56**, 1-28.

544 Qian, S. S., T. F. Cuffney, I. Alameddine, G. McMahon, and K. H. Reckhow (2010), On the
545 application of multilevel modeling in environmental and ecological studies. *Ecology*, **91**,
546 355-361.

547 R Core Team (2013) R: A language and environment for statistical computing. R Foundation
548 for Statistical Computing, Vienna, Austria. URL <http://www.R-project.org/>.

549 Schlesinger, W., and J. Andrews (2000), Soil respiration and the global carbon cycle. *Biogeo-*
550 *chemistry*, **48**, 7-20.

551 Schmidt, M. W. I., M. S. Torn, S. Abiven et al. (2011), Persistence of soil organic matter as
552 an ecosystem property. *Nature* **478**, 49-56.

553 Sierra, C. A., M. E. Harmon, and S. S. Perakis (2011), Decomposition of heterogeneous
554 organic matter and its long-term stabilization in soils. *Ecological Monographs*, **81**, 619-
555 634.

556 Singh, B. K., R. D. Bardgett, P. Smith, and D. Reay (2010), Microorganisms and climate
557 change: terrestrial feedbacks and mitigation options. *Nature Reviews Microbiology* **8**,
558 779-790.

559 Sinsabaugh, R.L., S. Manzoni, D. L. Moorhead, and A. Richter (2013) Carbon use efficiency
560 of microbial communities: stoichiometry, methodology and modelling *Ecology Letters* **16**
561 930-939.

562 Skjemstad, J., and L. R. Spouncer (2003), Integrated Soils Modelling for the National Carbon
563 Accounting System:(estimating Changes in Soil Carbon Resulting from Changes in Land
564 Use). (Australian Greenhouse Office).

565 Smith, J., P. Smith, M. Wattenbach et al. (2005), Projected changes in mineral soil carbon of
566 European croplands and grasslands, 1990-2080. *Global Change Biology*, **11**, 2141-2152.

567 Smith, J., P. Smith, M. Wattenbach et al. (2007), Projected changes in the organic carbon
568 stocks of cropland mineral soils of European Russia and the Ukraine, 1990–2070. *Global*
569 *Change Biology*, **13**, 342-356.

570 Smith, P., J. U. Smith, D. S. Powlson et al. (1997), A comparison of the performance of nine
571 soil organic matter models using datasets from seven long-term experiments. *Geoderma*,
572 **81**, 153-225.

573 Soetaert, K., and P. M. Herman PM (2008) A practical guide to ecological modelling: using
574 R as a simulation platform. (Springer).

575 Tang, J., and Q. Zhuang (2008), Equifinality in parameterization of process-based
576 biogeochemistry models: A significant uncertainty source to the estimation of regional
577 carbon dynamics. *Journal of Geophysical Research-Biogeosciences*, **113**, G04010.

578 Thorburn, P. J., M. E. Probert, and F. A. Robertson (2001), Modelling decomposition of
579 sugar cane surface residues with APSIM-residue. *Field Crop Research* **70**, 223-232.

580 Thornton, P.E., J. F. Lamarque, N. A. Rosenbloom, and N. M. Mahowald (2007), Influence
581 of carbon-nitrogen cycle coupling on land model response to CO₂ fertilization and climate
582 variability. *Global Biogeochemical Cycles*, **21**, GB4018.

583 Todd-Brown, K. E. O., Randerson, J. T., Post, W. M., Hoffman, F. M., Tarnocai, C., Schuur,
584 E. A. G., and Allison, S. D. (2013), Causes of variation in soil carbon simulations from
585 CMIP5 Earth system models and comparison with observations. *Biogeosciences*, **10**,
586 1717–1736

587 Wang, E., Robertson, M.J., Hammer, G.L., Carberry, P.S., Holzworth, D., Meinke, H.,
588 Chapman, S.C., Hargreaves, J.N.G., Huth, N.I., McLean, G., 2002. Development of a
589 generic crop model template in the cropping system model APSIM. *European Journal of*
590 *Agronomy*, **18**, 121-140.

591 Weng, E., and Y. Luo (2011), Relative information contributions of model vs. data to short-
592 and long-term forecasts of forest carbon dynamics. *Ecological Applications* **21**, 1490-
593 1505.

594 Xia, J., Y. Luo, Y. P. Wang, O. Hararuk (2013), Traceable components of terrestrial carbon
595 storage capacity in biogeochemical models. *Global Change Biology*, **19**, 2104-2116.

596 Xu, X., J. P. Schimel, P. E. Thornton, X. Song, F. M. Yuan, and S. Goswami (2014),
597 Substrate and environmental controls on microbial assimilation of soil organic carbon: a
598 framework for Earth system models. *Ecology Letters*, **17**, 547-555.

599 Zhou, J., K. Xue, J. P. Xie et al. (2012), Microbial mediation of carbon-cycle feedbacks to
600 climate warming. *Nature Climate Change*, 106-110.

601 **Table 1.** The effects of experiment-specific variance of model parameters and climate on
 602 individual-level coefficients (i.e., α_j^{expt} and β_j^{expt} in Fig. 4a).

Factor [†]	α^{expt}				β^{expt}			
	Estimate	SE	t value	P	Estimate	SE	t value	P
Model intercept	26.35	2.14	12.30	***	1.62	0.33	4.89	***
GV	3.15	0.55	5.69	***	0.17	0.088	1.97	•
R	-0.059	0.016	-3.63	***	-0.0055	0.0026	-2.15	*
T	4.95	1.35	3.66	***	-0.16	0.21	-0.77	0.44
GV × R	–	–	–	–	-0.0018	0.00061	-2.87	**
GV × T	-0.57	0.33	-1.74	•	–	–	–	–
R × T	-0.046	0.010	-4.49	***	0.0021	0.0014	1.46	0.15
Whole model R²		0.44		***		0.21		***

603 ***, P < 0.001; **, P < 0.01; *, P < 0.05; •, P < 0.1.

604 [†]GV, generalized variance of the identified three model parameters including microbial
 605 carbon use efficiency, decomposition rate of humic organic carbon and the fraction of inert
 606 organic carbon; R, the annual average rainfall; T, the annual average temperature. GV was
 607 logarithmically transformed and centered, and R and T were also centered when fitting the
 608 model.

609

610 **Figure legends**

611 **Figure 1.** Model performance in simulating soil organic carbon (SOC) dynamics (a) and the
612 corresponding optimized model parameters (b) across the studied 90 experiments. Circles and
613 bars (a) indicate the average and 95% confidence interval of the simulations for each
614 experiment using different parameter ensembles. Red and blue symbols in (a) highlight the
615 data at Tarlee and Brigalow respectively, corresponding to the data in Fig. 2. Dashed line is
616 the 1:1 line in (a). The parameter ensembles at Tarlee and Brigalow are highlighted in (b).
617 See Fig.2 for the means of the colorful symbols in (b), showing the different ranges of
618 optimized fraction of inert organic carbon (*finert*).

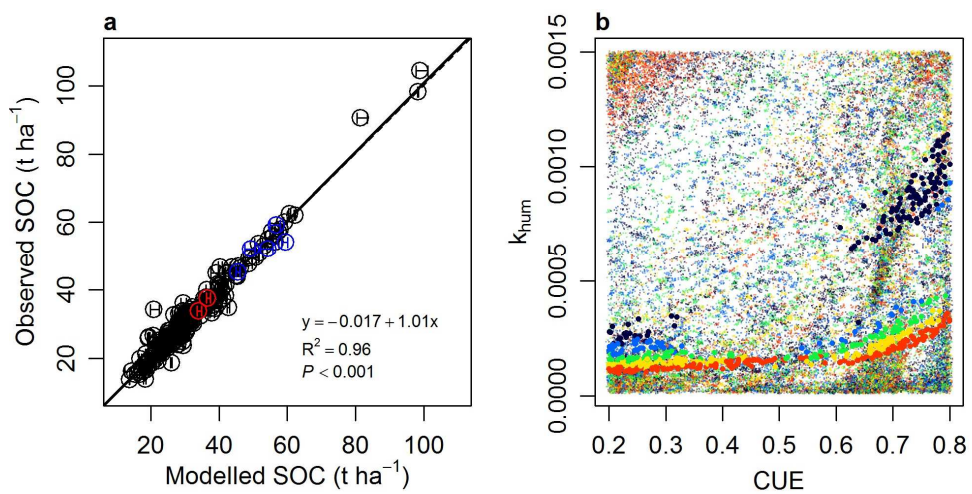
619 **Figure 2.** Projected soil organic carbon dynamics at two case sites Tarlee (a) and Brigalow (b)
620 and the correspondingly used parameter ensembles (c and d). Black symbols show the
621 observations. Seven criteria (RMSE, MAE, pMAE, IoA, rIoA, NSE and rNSE, see Table 3 in
622 the supplement for details) are used to derive the posterior joint distribution of model
623 parameters (*CUE*, *k_{hum}* and *finert*). *CUE*, microbial carbon use efficiency; *k_{hum}*, the potential
624 decomposition rate of humic organic carbon; *finert*, the fraction of inert organic carbon.

625 **Figure 3.** Projected SOC (a and b) and its percentage uncertainty (c and d) under high (a and
626 c) and low (b and d) carbon input scenarios after 100-year simulations in 90 experiments
627 across 26 sites. Concentric circles show the different experiments at the same site. The sizes
628 of the pies correspond to the projected average of SOC content (a and b) and the
629 corresponding percentage uncertainty (c and d). Blue and red circles indicate that the average
630 of the 700 simulations is increased and decreased, respectively, compared with the SOC
631 content at the start of the projection. Blue and red sectors of the pies in (c) and (d) indicate
632 the fraction of 700 bootstrapping simulations that shows an increase and a decrease of the
633 projected SOC, respectively, compared with the SOC content at the start of the projection

634 period.

635 **Figure 4.** Coefficients (estimate \pm standard deviation) for the regression model: $U_P = \alpha + \beta$
636 C_R . The model is fitted to estimate the effects of carbon input (C_R) on the percentage
637 uncertainty (U_P) in soil organic carbon projections, applied to 90 experiments (a) and 100
638 time-spans of projection (b). $\hat{\alpha}$, $\hat{\beta}$ and σ show the data-level coefficients (i.e., averaging over
639 experiments and time-spans of projection) and errors, respectively. In (a), experiments are
640 sorted according to α_j^{expt} . The coefficients at the experiment \times time-span level are not shown.
641 See more details in the Methods for the regression model.

642 Figure 1



643

